Random and Systematic Uncertainties of Reflection-Type Q-Factor Measurement With Network Analyzer

Darko Kajfez, *Life Senior Member, IEEE*

***Abstract*—The reflection-type measurement of the unloaded Q factor of microwave resonant cavities consists of measuring the complex reflection coefficient with a network analyzer as a function of frequency and fitting the measured data to a circle on a complex plane. The measurement errors are of two kinds: random errors caused by imperfect data fit to an ideal circle and systematic errors caused by the limited accuracy of the network analyzer and its accessories. This paper presents the methods for estimating the measurement uncertainties for both kinds of errors.**

***Index Terms*—Cavity resonators, measurement uncertainties, network analyzers, Q-factor measurement.**

I. Introduction

THE measurement of a Q factor by reflection-type method determines the loaded and unloaded Q factors by fitting the measured data to the so-called Q circle [1], [2]. Before the era of automatic network analyzers and personal computers, the measurement was performed with a slotted line and the data fitting was performed graphically, using a compass and a ruler [3]. Today, the measurement is performed with a vector network analyzer and the data fitting is accomplished numerically on a personal computer [4]–[8]. Accurate knowledge of the unloaded Q factor is important in measurement of material properties such as the surface resistivity of high-temperature superconductors [9] or the loss tangent of engine oil [10].

As with any scientific measurement, it is of importance to establish the accuracy of the measurement method. This paper will discuss the uncertainty limits of the reflection-type measurement, which is performed with an automatic vector network analyzer. Two types of errors will be discussed: random and systematic errors. The random errors cause the recorded data to depart from an ideal Q circle. The systematic errors are the reason for the worst case residual uncertainties such as specified by the manufacturers of network analyzers.

II. Random Errors

A. Data-Fitting Procedure

The data-processing procedure discussed here consists of fitting the measured complex reflection coefficient Γ to the ideal Q circle specified by a fractional linear transformation [7]

$$\Gamma = \frac{a_1 t + a_2}{a_3 t + 1}. \tag{1}$$

Manuscript received January 4, 2002.

The author is with the Department of Electrical Engineering, University of Mississippi, University, MS 38677 USA (e-mail: eedarko@olemiss.edu).

Digital Object Identifier 10.1109/TMTT.2002.807831

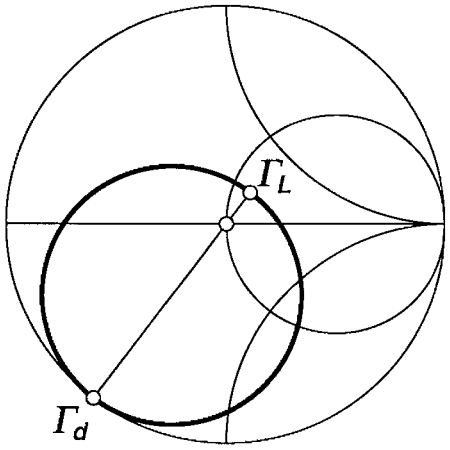

Fig. 1. Ideal Q circle (bold line) of a microwave resonator. The detuned reflection coefficient is denoted Γ_d and the loaded reflection coefficient is denoted Γ_L.

The real variable t is a normalized frequency variable

$$t = 2\,\frac{f - f_L}{f_0} \tag{2}$$

where f is the operating frequency, f_0 is the resonant frequency of the unloaded resonator, and f_L is the resonant frequency of the loaded resonator. For high-Q resonators (say, $Q > 100$), no loss of accuracy is committed by substituting f_L in place of f_0 in the denominator of (2) [11, p. 55].

The three complex coefficients a_1, a_2, and a_3 are the transformation constants that determine the properties of the fractional linear transformation. When the operating frequency is far from the resonant frequency, the corresponding reflection coefficient becomes $\Gamma_d = a_1/a_3$, i.e., the detuned reflection coefficient. On the other hand, when $f = f_L$, the reflection coefficient becomes $\Gamma_L = a_2$, i.e., the loaded reflection coefficient. The situation is illustrated in Fig. 1, which can be interpreted by the equivalent circuit shown in Fig. 2. In that circuit, R_c is equal to the characteristic impedance of the input port and X_s denotes the reactance of the coupling mechanism. The network analyzer is represented by a Thevenin source with internal impedance equal to R_c. The unloaded resonator is shown as a parallel resonant circuit characterized by Q_0, R_0, and $\omega_0 = 2\pi f_0$. When the coupling is capacitive, the Q circle is situated below the real axis (as shown in Fig. 1), and when it is inductive, the Q circle is situated above the real axis. However, if there is a section of a transmission line inserted between the resonator and external observation port, such as shown in Fig. 2, the circle may be rotated anywhere within the Smith chart.

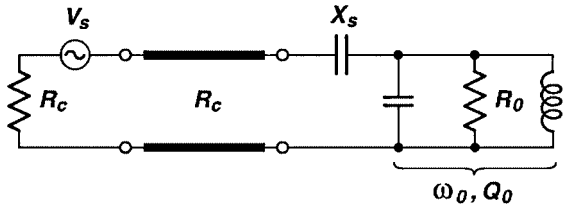

Fig. 2. Equivalent circuit for a reflection-type measurement of the Q factor.

The equivalent circuit shown here ignores the losses in the coupling mechanism in order to simplify the discussion of measurement uncertainty. In this case, Γ_d is located on the perimeter of the Smith chart (i.e., $|\Gamma_d| = 1$). Furthermore, the coefficient a_3 is pure imaginary, its magnitude being equal to the loaded Q factor [7]

$$Q_L = \mathrm{Im}(a_3). \tag{3}$$

The diameter of the Q circle is the distance between Γ_d and Γ_L

$$d = \left| a_2 - \frac{a_1}{a_3} \right|. \tag{4}$$

This diameter determines the value of the coupling coefficient [7]

$$\kappa = \frac{1}{\dfrac{2}{d} - 1}. \tag{5}$$

Knowing Q_L and κ, one can find the unloaded reflection coefficient Q_0 [3]

$$Q_0 = Q_L(1 + \kappa). \tag{6}$$

Clearly, once the transformation constants a_1 to a_3 are determined, the circuit elements Q_L, κ, and Q_0 are uniquely specified. The procedure of finding the transformation coefficients and their uncertainties is described in [11]. The starting point is to rewrite (1) in the implicit form

$$a_1 t + a_2 - a_3 t\Gamma = \Gamma. \tag{7}$$

The network analyzer measures the reflection coefficient Γ_n ($n = 1, \ldots, N$) at a number of frequency points f_1 to f_N. The corresponding normalized frequency variable t_n ($n = 1, \ldots, N$) is computed by (2). Each measured point yields an equation of type (7). In this way, one obtains a linear system of N equations that has to be solved for the three unknown transformation coefficients. In matrix notation, the system can be written as

$$a_1|e_1\rangle + a_2|e_2\rangle + a_3|e_3\rangle = |\Gamma\rangle \tag{8}$$

where $|e_1\rangle$ is a column vector containing the values t_1 to t_N, $|e_2\rangle$ is a vector that has all its components equal to unity, etc. The details may be found in [11, pp. 69–72]. To solve the system in the least square sense, one creates the projections of (8) onto directions of $|e_1\rangle$, $|e_2\rangle$, and $|e_3\rangle$, to obtain a 3×3 matrix equation

$$\boldsymbol{C}|a\rangle = |g\rangle. \tag{9}$$

The elements of matrix $\boldsymbol{C}$ are the weighted scalar products of the type

$$C_{ij} = \langle e_i|\boldsymbol{P}|e_j\rangle. \tag{10}$$

$|a\rangle$ is a column vector containing the three transformation constants and $|g\rangle$ is the column vector as follows:

$$|g\rangle = \begin{pmatrix} \langle e_1|\boldsymbol{P}|\Gamma\rangle \\ \langle e_2|\boldsymbol{P}|\Gamma\rangle \\ \langle e_3|\boldsymbol{P}|\Gamma\rangle \end{pmatrix}. \tag{11}$$

The diagonal matrix $\boldsymbol{P}$ contains the weights of individual measurements. Those weights are inversely proportional to the variances of individual measurements. The computational procedure must be performed iterative. In the first iteration, the weights are

$$p_n = \frac{1}{1 + t_n^2\left(1 + |\Gamma_n|^2\right)}. \tag{12}$$

In the later iteration steps, the computation of weights is specified in Section II-B. When the iteration is finished, the three unknown coefficients are obtained by inverting the matrix equation (9)

$$|a\rangle = \boldsymbol{D}|g\rangle \tag{13}$$

where $\boldsymbol{D} = \boldsymbol{C}^{-1}$.

B. Uncertainties Due to Random Errors

To determine the variances of the transformation coefficients, one substitutes the computed values of the transformation coefficient back into (8). The nth line of this equation system yields a remaining error

$$\varepsilon_n = a_1 t_n + a_2 - a_3 t_n \Gamma_n - \Gamma_n. \tag{14}$$

The weighted squared sum of errors is a real number

$$S^2 = \sum_{n=1}^{N} p_n |\varepsilon_n|^2. \tag{15}$$

Using this quantity, the variances of transformation coefficients are computed as follows [11, p. 81]:

$$\sigma^2(a_m) = \frac{D_{mm} S^2}{\sum\limits_{j=1}^{3} C_{jj} D_{jj}}. \tag{16}$$

Although the transformation coefficients are complex numbers, their deviation is expressed here with a real number. It is assumed that the real and imaginary parts of complex numbers have the same variances and that they are uncorrelated. In that case, the uncertainty (= standard deviation = square root of variance) is a real number that defines the radius of a circle on the complex plane, which contains about 63% of points with normal random distribution [12, p. 195]. This value is not far from 68% that goes with the "standard deviation" commonly used for specifying the experimental uncertainty of real variables.

For the second and third iteration, more accurate weights are computed as follows [11, p. 74]:

$$p_n = \frac{1}{t_n^2\sigma^2(a_1) + \sigma^2(a_2) + t_n^2|\Gamma_n|^2\sigma^2(a_3)}. \tag{17}$$

No more than three iterations are needed [11, p. 99] so that the computational procedure is almost instant, even if one measures 1601 data points (the maximum that the network analyzer can take).

Starting with the transformation constants and their variances evaluated as above, the values of the circuit elements and their uncertainties are obtained in a straightforward manner. As the unloaded Q depends only on a_3, the uncertainty (standard deviation) of Q_L is

$$\sigma(Q_L) = \sigma(a_3). \tag{18}$$

The diameter d of the Q circle depends on all three transformation coefficients according to (4). By using the error propagation formula for random quantities [13, p. 114]

$$\sigma^2(d) = \left|\frac{\partial d}{\partial a_1}\right|^2 \sigma^2(a_1) + \left|\frac{\partial d}{\partial a_2}\right|^2 \sigma^2(a_2) + \left|\frac{\partial d}{\partial a_3}\right|^2 \sigma^2(a_3) \tag{19}$$

one obtains the uncertainty of d

$$\sigma(d) = \sqrt{\frac{\sigma^2(a_1)}{|a_3|^2} + \sigma^2(a_2) + \left|\frac{a_1}{a_3^2}\right|^2 \sigma^2(a_3)}. \tag{20}$$

As the coupling coefficient depends only on d, its uncertainty is given by

$$\sigma(\kappa) = \frac{2\sigma(d)}{(2-d)^2}. \tag{21}$$

The uncertainty of Q_0 follows from (6)

$$\sigma(Q_0) = \sqrt{(1+\kappa)^2\sigma^2(Q_L) + Q_L^2\sigma^2(\kappa)}. \tag{22}$$

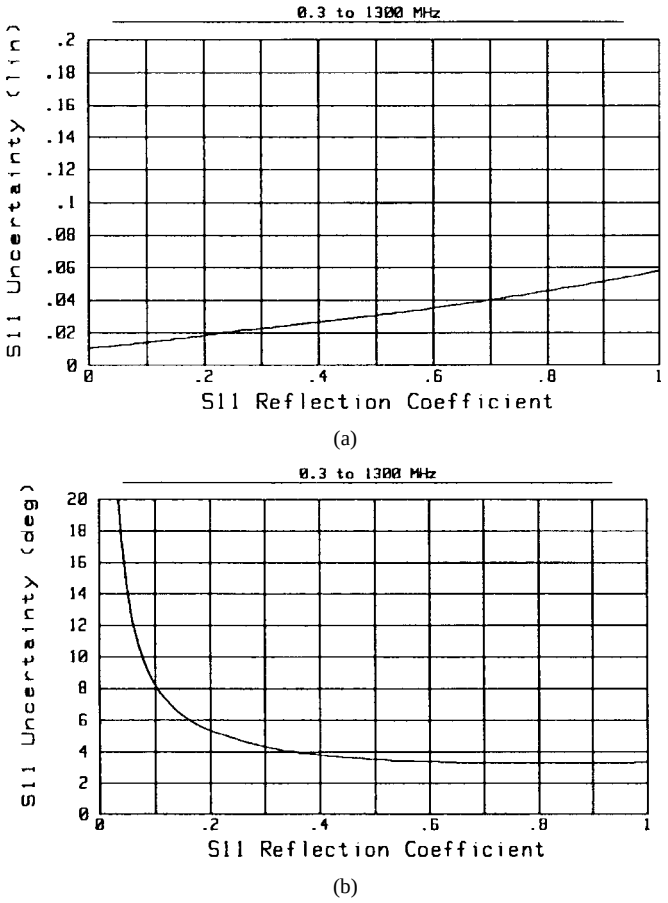

Fig. 3. Residual error specification for Agilent Network Analyzer Model 8712C (see [14]). (a) Amplitude uncertainty. (b) Phase uncertainty.

III. Systematic Errors

A. Instrument Error Specifications

Most network analyzers can measure all four scattering parameters of a two-port, but here, we are interested only in the measurement of S_{11}, i.e., the reflection coefficient of a one-port. Two important technical specifications of the network analyzer that influence the accuracy of the Q factor measurement are: 1) the source mismatch and 2) the residual S_{11} uncertainty. The source mismatch is a measure of how much the internal impedance of the network analyzer departs from its nominal value of 50 Ω. The mismatch is expressed in decibels (return loss); typical values range between 30–40 dB. The residual uncertainty describes the worst case departure from the correct value that can be expected from a given model of a network analyzer after it has been properly calibrated. For the model HP8712C, the S_{11} residual amplitude and phase uncertainties are shown in Fig. 3(a) and (b) [14].

It is seen from Fig. 3(a) that the magnitude uncertainty of the reflection coefficient is smallest at the center of the Smith chart, where it has a value of ± 0.01. The uncertainty grows when the measured point moves toward the perimeter of the Smith chart, where it attains the value of ± 0.06. Therefore, in the worst case, the displayed reflection coefficient of a lossless one-port can be as large as 1.06, while the network analyzer is still working within specifications. This is quite a large error, but fortunately, the observed error in experiments to be described in Section IV was never that large. The largest value of the detuned reflection coefficient Γ_d (i.e., the point farthest away from the center of the Smith chart) was only 1.4% larger than unity.

Although not obvious from Fig. 3(a) and (b), the phase uncertainty is related to the magnitude uncertainty. If one assumes that the complex number Γ can take an arbitrary value within a circle of radius $\Delta|\Gamma|$, then the maximum phase error is $\tan\Delta\varphi = \Delta|\Gamma|/|\Gamma|$ (see Fig. 4). Within the accuracy of reading Fig. 3(a) and (b), this relationship holds true for all the points, except $|\Gamma| = 0$, where the phase is irrelevant anyway. It is, therefore, concluded that, for the purpose of estimating the systematic uncertainty of the complex number S_{11}, one can assume both the amplitude and phase errors to be described by a single real number, which is equal to the amplitude uncertainty $\Delta|\Gamma|$. In the examples that follow, the values of $\Delta|\Gamma|$ were read from the manufacturer's diagrams and stored in the form of data tables, one for each frequency range specified by the manufacturer. The computational procedure for evaluation of systematic errors then linearly interpolates the values between the tabulated data for a specific network analyzer. The phase uncertainty curves are not used in the procedure described in this paper, as they are deemed superfluous.

B. Uncertainties Due to Source Mismatch

To simplify the discussion, the length of the transmission line in the equivalent circuit in Fig. 2 will be shrunk to zero. The

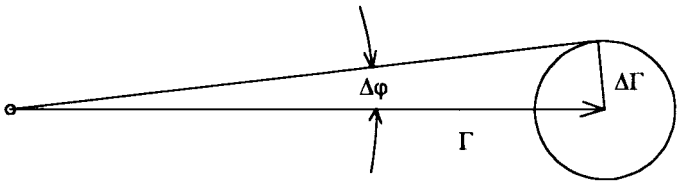

Fig. 4. Uncertainty circle on the complex plane Γ.

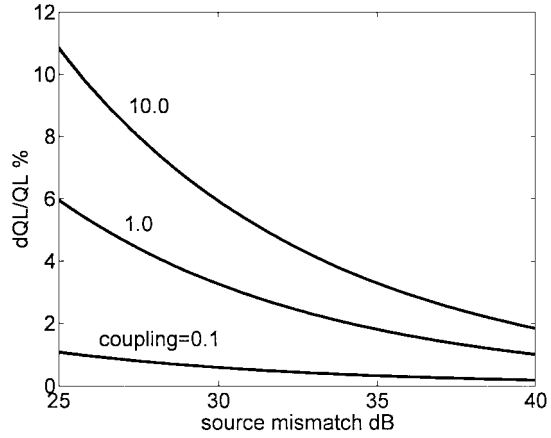

Fig. 5. Relative error in loaded Q due to the source mismatch.

computed conductance of the external circuit that is connected in parallel with the unloaded resonator becomes [11, p. 91]

$$G_{\text{ex}} = \frac{R_c}{R_c^2 + X_s^2}. \tag{23}$$

The coupling coefficient κ is the ratio of the power dissipated in the external circuit to the power dissipated in the unloaded resonator

$$\kappa = G_{\text{ex}} R_0 = \frac{R_0}{R_c\left(1 + \left(\frac{X_s}{R_c}\right)^2\right)}. \tag{24}$$

When the source resistance R_c is in error by a small amount δR_c, the corresponding error in the coupling coefficient is

$$\delta\kappa = \frac{d\kappa}{dR_c}\,\delta R_c = -\kappa_0 \frac{1 - \left(\frac{X_s}{R_c}\right)^2}{1 + \left(\frac{X_s}{R_c}\right)^2} \cdot \frac{\delta R_c}{R_c} \tag{25}$$

where the unperturbed value of the coupling coefficient was denoted κ_0. It follows from the above expression that, for any value of X_s, the relative error of the coupling coefficient cannot be larger than the relative error of the source resistance

$$\left|\frac{\delta\kappa}{\kappa_0}\right|_{\max} = \left|\frac{\delta R_c}{R_c}\right|. \tag{26}$$

The corresponding increment in Q_L is

$$\delta Q_L = \left.\frac{dQ_L}{d\kappa}\right|_{\kappa=\kappa_0} \delta\kappa. \tag{27}$$

Applied to (6), this gives

$$\left|\frac{\delta Q_L}{Q_L}\right| = \frac{1}{1 + \frac{1}{\kappa_0}} \cdot \left|\frac{\delta R_c}{R_c}\right|. \tag{28}$$

The source mismatch (the manufacturer prefers to call this quantity "source match") of the network analyzer is expressed as follows:

$$\frac{\delta R_c}{R_c} = \frac{2}{10^{\alpha/20} - 1} \tag{29}$$

where α is the mismatch return loss in decibels.

The last two equations can be used to find the uncertainty of the measured value of Q_L as a function of the source mismatch δR_c. As seen from (28), the nominal value of the coupling coefficient κ_0 plays an important role: small values of the coupling coefficient greatly reduce the uncertainty of Q_L. This situation is illustrated in Fig. 5. It can be seen that, as long as the coupling coefficient is smaller than 0.1, the uncertainty in Q_L is smaller than 1% even for a network analyzer with a poor mismatch of $\alpha = 25$ dB. However, for a critically coupled resonator ($\kappa_0 = 1$), the uncertainty in Q_L is smaller than 1% only for a very well-matched network analyzer with $\alpha = 40$ dB. For a strong coupling of $\kappa_0 = 10$, even the best-matched network analyzer cannot guarantee an uncertainty in Q_L smaller than 2%.

Once the uncertainties δQ_L and $\delta\kappa$ are known, the worst case uncertainty of the unloaded Q, due to the source mismatch of the network analyzer, follows from (6) as

$$\delta Q_0 = \left|\frac{\partial Q_0}{\partial Q_L}\,\delta Q_L\right| + \left|\frac{\partial Q_0}{\partial \kappa}\,\delta\kappa\right| = (1+\kappa)\,|\delta Q_L| + Q_L\,|\delta\kappa|. \tag{30}$$

C. Uncertainties Due to Residual Errors

The residual error in the measured value S_{11} (denoted here by Γ) may distort the apparent diameter of the Q circle. According to Fig. 1, diameter d is equal to the distance between the reflection coefficients Γ_d and Γ_L. The residual errors for two close points on the Smith chart most probably point in the same direction. Thus, if the Q circle is very small, both points Γ_d and Γ_L are likely to be shifted in the same direction so that the diameter of the Q circle is not at all affected by the residual error. On the other hand, for a very strongly coupled resonator, d approaches the value of two and the points Γ_d and Γ_L are located on diametrically opposite sides of the Smith chart. It will be assumed here that, in such a case, the phase of $\Delta\Gamma_d$ is opposite to the phase of $\Delta\Gamma_L$ so that the error in d is a sum of the magnitudes $|\Delta\Gamma_d|$ and $|\Delta\Gamma_L|$ (worst case). In between these two extremes, the phase will be assumed to grow proportionally with d so that the worst case uncertainty of d, caused by the residual error of the network analyzer, is expressed as follows:

$$\Delta d = |\Delta\Gamma_d| - |\Delta\Gamma_L| \cos\left(\pi\,\frac{d}{2}\right). \tag{31}$$

The values of $|\Delta\Gamma_d|$ and $|\Delta\Gamma_L|$ are read from the curves, such as in Fig. 3(a), which is provided by the manufacturer of the

network analyzer. The uncertainty in the coupling coefficient is then obtained from (5)

$$\Delta\kappa = \frac{\partial\kappa}{\partial d}\,\Delta d = \frac{2}{(2-d)^2}\,\Delta d. \tag{32}$$

For overcritically coupled resonators, the denominator of (32) becomes smaller than unity so that even a small error in diameter can cause a large uncertainty in the coupling coefficient and, hence, a large uncertainty in Q_0. For instance, for $\kappa = 10$, $\Delta\kappa = 60.5\Delta d$, whereas for $\kappa = 0.1$, one has only $\Delta\kappa = 0.605\Delta d$. Therefore, for an accurate measurement of the unloaded Q, the resonator should be undercritically coupled in order to minimize the role of the residual network-analyzer error. A similar conclusion was obtained in the Section III-B, when discussing the error caused by the source mismatch of the network analyzer.

To estimate the uncertainty in Q_L, one assumes that the reflection coefficient has been changed by an incremental value $\Delta\Gamma$. As a consequence, the transformation constants a_1 to a_3 will also have changed by small amounts. Equation (8) will then be modified as follows:

$$(a_1+\Delta a_1)|e_1\rangle + (a_2+\Delta a_2)|e_2\rangle + (a_3+\Delta a_3)|e_3+\Delta e_3\rangle = |\Gamma+\Delta\Gamma\rangle. \tag{33}$$

Subtracting (8) from (33) and performing the weighted scalar products, one obtains the normal system of equations for the first-order increments of transformation constants

$$\boldsymbol{C}|\Delta a\rangle = |\Delta g\rangle \tag{34}$$

where

$$|\Delta g\rangle = \begin{pmatrix} \langle e_1|\boldsymbol{P}|\Delta\Gamma\rangle - a_3\langle e_1|\boldsymbol{P}|\Delta e_3\rangle \\ \langle e_2|\boldsymbol{P}|\Delta\Gamma\rangle - a_3\langle e_2|\boldsymbol{P}|\Delta e_3\rangle \\ \langle e_3|\boldsymbol{P}|\Delta\Gamma\rangle - a_3\langle e_3|\boldsymbol{P}|\Delta e_3\rangle \end{pmatrix}. \tag{35}$$

The estimates Δa_1, Δa_2, and Δa_3 can be evaluated by using $\boldsymbol{D}$, the inverse of the system matrix evaluated earlier in the process of data fitting

$$|\Delta a\rangle = \boldsymbol{D}|\Delta g\rangle. \tag{36}$$

The weighted scalar products from (35) result in the following explicit components of $|\Delta g\rangle$:

$$\Delta g_1 = \sum_{n=1}^{N} p_n(t_n + a_3 t_n^2)\Delta\Gamma_n \tag{37}$$

$$\Delta g_2 = \sum_{n=1}^{N} p_n(1 + a_3 t_n)\Delta\Gamma_n \tag{38}$$

$$\Delta g_3 = -\sum_{n=1}^{N} p_n(1 + a_3 t_n)t_n\Gamma_n^*\Delta\Gamma_n. \tag{39}$$

The amplitudes of $\Delta\Gamma_n$ are determined from the residual uncertainty curves, such as in Fig. 3(a). The phase is postulated to grow proportionally to the projection of the vector $(\Gamma_d - \Gamma_n)$ onto Γd. Therefore, for small Q circles, the phase of $\Delta\Gamma_n$ remains small for all the points, whereas for large Q circles, the maximum phase approaches the value of π radians. Such a phase behavior is consistent with the one specified by (31). Only the third row of (36) is needed for evaluation of ΔQ_L as follows:

$$\Delta Q_L = |\Delta a_3|. \tag{40}$$

The worst case uncertainty in Q_0, due to residual error of the network analyzer, is then

$$\Delta Q_0 = (1+\kappa)\Delta Q_L + Q_L\Delta\kappa. \tag{41}$$

IV. Validation Measurements and Discussion

The uncertainties evaluated in Section II are of a different nature than those evaluated in Section III. For random errors, the standard uncertainty means a 63% probability that the complex number will be situated within the specified error circle. For systematic errors, the uncertainty means that the worst-case result will be within the specified error limits. It is reasonable to assume that most-probable systematic uncertainties will be considerably smaller than the worst case uncertainties. In order to compare the systematic uncertainties with the random uncertainties, the "quasi-standard" systematic uncertainties here will be made equal to one-third of the worst case systematic uncertainties evaluated in Section III. This means that we trust the manufacturer to be capable of delivering 99.7% of his instruments with smaller than the worst case uncertainties. For a normal random distribution, such a percentage is associated with three times the standard uncertainty [13, p. 174]. For instance, the overall uncertainty of Q_0, including both the random and systematic errors, will be computed as

$$\sigma_{\rm tot}(Q_0) = \sqrt{\sigma^2(Q_0) + \left(\frac{1}{3}\,\delta Q_0\right)^2 + \left(\frac{1}{3}\,\Delta Q_0\right)^2} \tag{42}$$

where $\sigma(Q_0)$ is given by (22), δQ_0 is given by (30), and ΔQ_0 is given by (41). The overall uncertainties $\sigma_{\rm tot}(Q_L)$ and $\sigma_{\rm tot}(\kappa)$ will be expressed in an analogous fashion.

Fig. 6 shows the resonator that was used in these measurements. Inside the copper-plated cavity is a dielectric resonator of a tubular shape, with a dielectric tuning post. The operating frequency can be tuned in the vicinity of 900 MHz. The resonator was intended as a filter between a transmitter and the antenna so it contains two coaxial ports. Inside the cavity, each coaxial connector is coupled to the resonator with a short loop. The principal purpose of the experiments to be described is to establish the value of the unloaded Q factor Q_0 and its uncertainty.

The coaxial connectors are mounted by three machine screws each and are easy to rotate (for adjusting the coupling coefficient). The coaxial connector at port 2 is next removed and replaced by a short-circuiting plate to prevent radiation. In this way, a one-port resonator is created at port 1. The orientation of the loop is selected such that the coupling is undercritical. Using the network analyzer model HP8712C, the resonance of the $\rm TE_{01\delta}$ mode was found around 944 MHz so the network analyzer was calibrated for the range of 941–947 MHz in 401

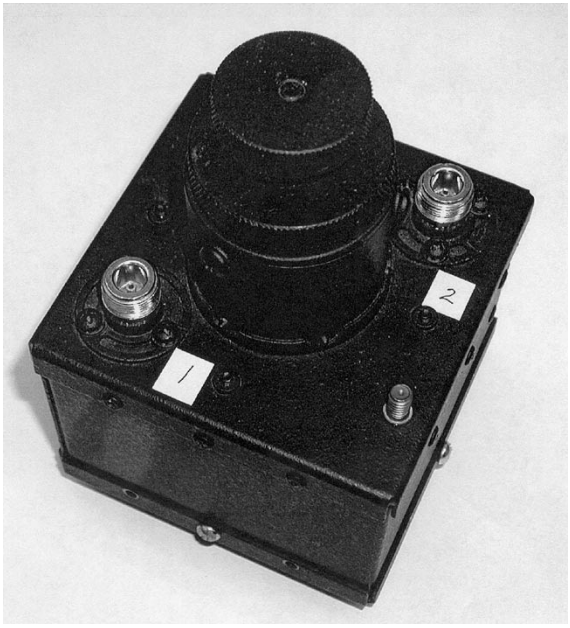

Fig. 6. Two-port resonator.

TABLE I
UNCERTAINTY ANALYSIS FOR SELECTED MEASUREMENTS

	Meas. #1 HP8712C	Meas. #2 HP8510C	Meas. #7 HP8712C	Meas. #8 HP8510C
Q_L	9536	9713	11287	11562
$\sigma(Q_L)$	47	29	53	44
$\frac{1}{3}\Delta Q_L$	67	20	70	22
$\frac{1}{3}\delta Q_L$	85	27	74	23
$\sigma_{tot}(Q_L)$	118	44	115	55
κ	0.6896	0.6983	0.4318	0.4333
$\sigma(\kappa)$	0.0103	0.0059	0.0068	0.0038
$\frac{1}{3}\Delta\kappa$	0.0252	0.0077	0.0146	0.0045
$\frac{1}{3}\delta\kappa$	0.0218	0.0067	0.0218	0.0067
$\sigma_{tot}(\kappa)$	0.0349	0.0118	0.0271	0.0089
Q_0	16111	16496	16160	16572
$\sigma(Q_0)$	126	75	108	76
$\frac{1}{3}\Delta Q_0$	354	108	266	85
$\frac{1}{3}\delta Q_0$	351	111	352	112
$\sigma_{tot}(Q_0)$	514	172	454	159

Notation: σ: standard uncertainty due to random error, δ: worst case uncertainty due to source mismatch, Δ: worst case uncertainty due to residual error.

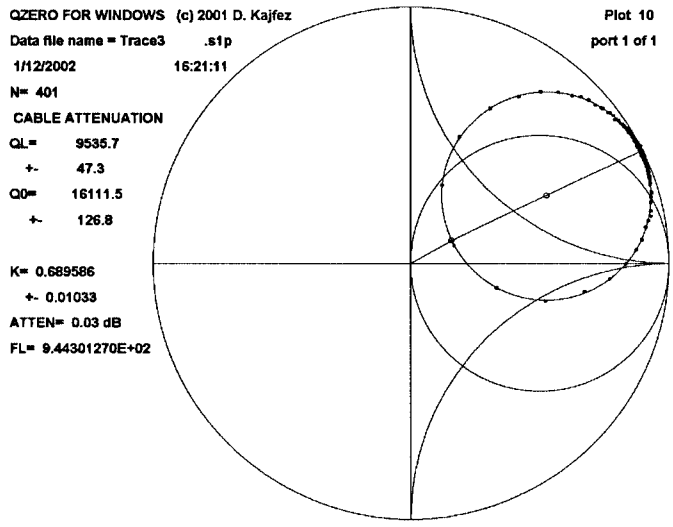

Fig. 7. Measurement #1, Smith chart display.

steps. The measured S_{11} data were then processed with the program *QZERO* for Windows.[1] As indicated in Section II-A, the losses in the coupling mechanism are ignored. This has been achieved by using the program option "CABLE ATTENUATION." The result of data processing is shown in Fig. 7. In the discussion that follows, this will be called measurement #1.

The unloaded Q was found to be 16 112 with the random uncertainty ± 127. The program *QZERO* only computes the uncertainty due to random deviation, using the procedure from Section II. This value does not include the uncertainty caused by the systematic errors of the network analyzer. The same resonator is then measured with the top-of-the-line network analyzer model HP8510C, calibrated for the same frequency range and the same number of points. When the measured data were processed with *QZERO* for Windows, the result for the unloaded Q was found to be $16\,497 \pm 75$. This is called measurement #2.

Next, the systematic uncertainties were computed by the procedure described above, and the results are summarized in Table I. A surprising fact is that the same resonator measured by different network analyzers yields different results for the loaded and unloaded Q factors, although the data are processed in the same way. The overall uncertainty $\sigma_{\rm tot}(Q_0)$ for model HP8712C is 3.2% and, for model HP8510C, it is considerably better, namely, 1.0%. These uncertainties include both the random and systematic errors. For both network analyzers, the systematic errors are more significant than the random errors. In each category of uncertainty contributions, model HP8712C accumulates the uncertainties two-to-three times larger than those for model HP8510C.

The ultimate goal of any Q factor measurement is to determine the unloaded Q, i.e., Q_0. This is an inherent property of the resonator and its value does not depend on the amount of coupling between the resonator and external circuit. Therefore, when the loop-and-connector assembly at port 1 is rotated, κ and Q_L should vary, but the value of Q_0 should remain constant. For a medium coupling, measurement #3 is performed with HP8712C, and measurement #4 is performed with HP8510C. In an analogous way, for the strongest coupling coefficient (at port 1), the corresponding measurements are denoted by #5 and #6. Afterwards, the coaxial coupling at port 1 was removed, and the opening was covered with a short-circuiting plate. The other coaxial connector-and-loop assembly was then inserted at port 2 and measurements #7–#12 were taken in an analogous way. Odd measurement numbers stand for HP8712C and even numbers stand for HP8510C. The coupling coefficients found in each measurement are shown in Table II.

[1]*QZERO* for Windows, Vector Forum, Oxford, MS. Software. Student version is distributed free to students and faculty at educational institutions by sending an e-mail message to eedarko@olemiss.edu. The full version may be obtained from Vector Forum via telephone at +1 662 234 4287.

TABLE II
COUPLING COEFFICIENTS OF INDIVIDUAL MEASUREMENTS

Measurement	κ_1	Measurement	κ_2
#1	0.690	#7	0.432
#2	0.698	#8	0.433
#3	1.153	#9	2.241
#4	1.173	#10	2.325
#5	4.074	#11	4.033
#6	4.278	#12	4.238

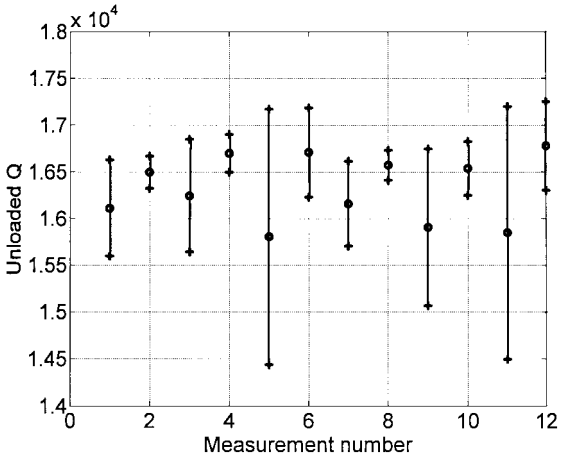

Fig. 8. Unloaded Q factors and their overall uncertainties. Odd numbered measurements: HP8712C. Even numbered measurements: HP8510C.

The results for Q_0 and its uncertainty are displayed in Fig. 8. The smallest uncertainty (approximately $\pm 1\%$) is obtained for measurements #2 and #8, which correspond to the smallest coupling at each port, both measured with HP8510C. For stronger coupling, the uncertainties increase. The largest uncertainty obtained with HP8510C is $\pm 2.8\%$ (measurement #6), corresponding to the strongest coupling. The values of Q_0 measured with HP8510C are all pretty consistent: the lowest result being 16 496 (#2) and the highest one being 16 780 (#12), differing by 1.7% from each other. The results obtained by HP8712C are scattered in a wider range, namely, from 15 806 (#5) to 16 246 (#3), i.e., within 2.7% from each other. The uncertainties are also larger than for the HP8510C, the smallest one being $\pm 2.8\%$ (#7) and the largest one being $\pm 8.6\%$ (#5).

Table I contains the four measurements utilizing an undercritical coupling, i.e., such as appropriate for minimizing the effect of systematic errors. The consistency of results for the unloaded Q measured from port 1 and the one measured from port 2 is remarkable in view of the fact that the two coupling coefficients differ considerably from each other (measurements #2 and #8). According to [15], such a difference in coupling coefficients would cause an additional uncertainty of $\pm 3.0\%$ if Q_0 was measured by the transmission-type method.

The problem remains that all the values of Q_0 obtained with model HP8712C are lower from those obtained with HP8510C. This is probably due to the source mismatch of HP8712C being only 30 dB, as compared with the value of 40 dB for the HP8510C. Nevertheless, the differences in results are within the estimated uncertainty limits.

V. CONCLUSIONS

The reflection-type method of measuring the Q factor consists of taking 50 or more points on the Smith chart as a function of frequency and fitting the measured data to an ideal circle. The reflection coefficients measured with the vector network analyzer are complex numbers. In this paper, the random error analysis is based on an assumption that a single real number can be defined, which signifies the 63% probability radius within which the complex point can be found.

Two kinds of measurement errors influence the overall uncertainty of the results: random and systematic errors. As far as the systematic errors are concerned, the source mismatch of the network analyzer is about as important as the residual S_{11} errors. The effect of both these errors can be minimized by using an undercritical coupling to the resonator. However, if the coupling is reduced too much, the Q circle becomes very small and the random S_{11} errors may dominate the overall uncertainty. It is believed that couplings between 0.1–1 are appropriate for a proper balance between random and systematic errors.

From the experiments conducted with the resonator at 940 MHz, it can be concluded that the network analyzer model HP8510C is capable of assuring the overall uncertainty of Q_0 at approximately 1%, and model HP8712C at approximately 3%, provided the resonator being tested is undercritically coupled.

The analytic expressions derived in this paper enable one to estimate the uncertainties caused by both random and systematic errors for each measured data set. Thus, it becomes possible for an experimentalist to process the measured data in a way that will determine not only the least-square values of Q_L, κ, and Q_0, but also their overall uncertainties for a specific network analyzer and for a given frequency of operation.

ACKNOWLEDGMENT

The dielectric-resonator cavity used in the experiments was donated by the Celwave Combiner Group, Phoenix, AZ.

REFERENCES

[1] W. Altar, "Q circles—A means of analysis of resonant microwave systems," *Proc. IRE*, vol. 35, pp. 355–361, Apr. 1947.
[2] W. Altar, "Q circles—A means of analysis of resonant microwave systems," *Proc. IRE*, vol. 35, pp. 478–484, May 1947.
[3] E. L. Ginzton, *Microwave Measurements*. New York: McGraw-Hill, 1957.
[4] W. P. Wheeless and D. Kajfez, "Experimental characterization of multimoded microwave resonators using automated network analyzer," *IEEE Trans. Microwave Theory Tech.*, vol. MTT-35, pp. 1263–1270, Dec. 1987.
[5] M. Sanchez, E. Martin, and J. Zamarro, "New vectorial automatic technique for characterization of resonators," *Proc. Inst. Elect. Eng.*, pt. H, vol. 136, pp. 145–150, Apr. 1989.
[6] C. P. Hearn, E. S. Bradshaw, and R. J. Trew, "The effect of coupling line loss in microstrip to dielectric resonator coupling," *Microwave J.*, vol. 33, pp. 169–178, Nov. 1990.
[7] D. Kajfez, "Linear fractional curve fitting for measurement of high Q factors," *IEEE Trans. Microwave Theory Tech.*, vol. 42, pp. 1149–1153, July 1994.
[8] K. Leong, J. Mazierska, and J. Krupka, "Measurements of unloaded Q-factor of transmission mode dielectric resonators," in *IEEE MTT-S Int. Microwave Symp. Dig.*, 1997, pp. 1639–1642.

[9] J. Mazierska, "Dielectric resonator as possible standard for characterization of high temperature superconducting films for microwave applications," *J. Superconduct.*, vol. 10, no. 2, pp. 73–84, 1997.
[10] D. Kajfez, M. Reed, and C. E. Smith, "Loss tangent of motor oil at 10 GHz," *Microwave Opt. Technol. Lett.*, vol. 21, no. 1, pp. 15–18, Apr. 5, 1999.
[11] D. Kajfez, *Q Factor*. Oxford, MS: Vector Forum, 1994.
[12] A. Papoulis, *Probability, Random Variables, and Stochastic Processes*. New York: McGraw-Hill, 1965.
[13] L. C. Parratt, *Probability and Experimental Errors in Science*. New York: Wiley, 1961.
[14] *HP8712 C and HP8714C RF Network Analyzers User's Guide*, Hewlett-Packard Company, Santa Rosa, CA, Feb. 1998.
[15] D. Kajfez, S. Chebolu, M. R. Abdul-Gaffoor, and A. A. Kishk, "Uncertainty analysis of the transmission-type measurement of Q-factor," *IEEE Trans. Microwave Theory Tech.*, vol. 47, pp. 367–371, Mar. 1999.

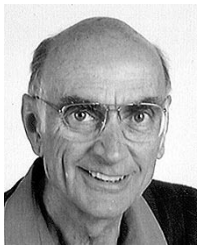

Darko Kajfez (SM'67–LS'98) received the Dipl.Ing. degree in electrical engineering from the University of Ljubljana, Ljubljana, Slovenia, in 1953, and the Ph.D. degree from the University of California at Berkeley, in 1967.

He is Emeritus Professor of Electrical Engineering at the University of Mississippi, University. He coedited *Dielectric Resonators* (Norwood, MA: Artech House, 1986; Oxford, MS: Vector Forum, 1990; Tucker, GA: Noble, 1998), authored the three-volume graduate textbook *Notes on Microwave Circuits* (Oxford, MS: Vector Forum, 1984, 1986, 1988), and the monograph *Q Factor* (Oxford, MS: Vector Forum, 1994). His research interests include RF and microwave measurement and analysis.